

Cytotoxicity of Quantum Dots Used for *In Vitro* Cellular Labeling: Role of QD Surface Ligand, Delivery Modality, Cell Type, and Direct Comparison to Organic Fluorophores

Christopher E. Bradburne,[†] James B. Delehanty,^{*,†} Kelly Boeneman Gemmill,[†] Bing C. Mei,[§] Hedi Mattoussi,[§] Kimihiro Susumu,^{§,‡} Juan B. Blanco-Canosa,^{||} Philip E. Dawson,^{||} and Igor L. Medintz^{*,†}

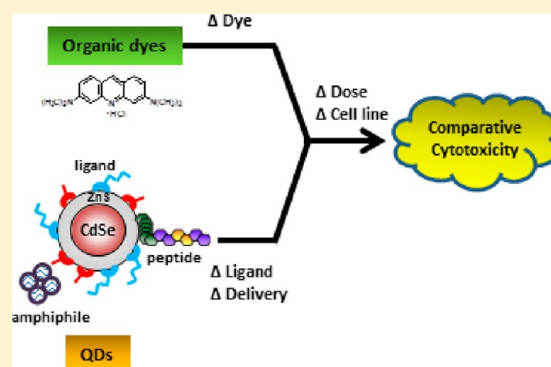
[†]Center for Bio/Molecular Science and Engineering, Code 6900, and [§]Optical Sciences Division, Code 5600, U.S. Naval Research Laboratory, Washington, DC 20375, United States

[‡]Sotera Defense Solutions, Annapolis Junction, Maryland 20701, United States

^{||}Departments of Cell Biology and Chemistry, The Scripps Research Institute, La Jolla, California 92037, United States

S Supporting Information

ABSTRACT: Interest in taking advantage of the unique spectral properties of semiconductor quantum dots (QDs) has driven their widespread use in biological applications such as *in vitro* cellular labeling/imaging and sensing. Despite their demonstrated utility, concerns over the potential toxic effects of QD core materials on cellular proliferation and homeostasis have persisted, leaving in question the suitability of QDs as alternatives for more traditional fluorescent materials (e.g., organic dyes, fluorescent proteins) for *in vitro* cellular applications. Surprisingly, direct comparative studies examining the cytotoxic potential of QDs versus these more traditional cellular labeling fluorophores remain limited. Here, using CdSe/ZnS (core/shell) QDs as a prototypical assay material, we present a comprehensive study in which we characterize the influence of QD dose (concentration and incubation time), QD surface capping ligand, and delivery modality (peptide or cationic amphiphile transfection reagent) on cellular viability in three human cell lines representing various morphological lineages (epithelial, endothelial, monocytic). We further compare the effects of QD cellular labeling on cellular proliferation relative to those associated with a panel of traditionally employed organic cell labeling fluorophores that span a broad spectral range. Our results demonstrate the important role played by QD dose, capping ligand structure, and delivery agent in modulating cellular toxicity. Further, the results show that at the concentrations and time regimes required for robust QD-based cellular labeling, the impact of our in-house synthesized QD materials on cellular proliferation is comparable to that of six commercial cell labeling fluorophores. Cumulatively, our results demonstrate that the proper tuning of QD dose, surface ligand, and delivery modality can provide robust *in vitro* cell labeling reagents that exhibit minimal impact on cellular viability.



INTRODUCTION

Cellular labeling with fluorescent molecules is a central technique in cell biology that continues to evolve with the advent of new fluorescent probes possessing unique properties and new methodologies for introducing them into cells. For example, the coupling of fluorescent proteins with molecular genetic engineering has enabled the real-time *in vitro* cellular tracking of individual molecules and intracellular macromolecular structures.^{1,2} Similarly, the discovery and development of novel materials such as cell-penetrating peptides (CPPs)^{3,4} for the delivery of fluorescent probes into cells has expanded the repertoire of tools available to investigate biochemical processes in live cells. Over the past 10 years, luminescent semiconductor nanocrystals, or quantum dots, (QDs) have received enormous attention as highly fluorescent probes with utility in *in vitro* labeling, imaging, and sensing applications.^{5–7} QDs cumulatively manifest several inherent

spectral properties that make them superior alternatives to more traditionally employed organic dyes and fluorescent proteins for direct fluorescent/multiphoton probing of cellular processes and as integral parts of Förster resonance energy transfer (FRET)-based sensors.^{5–14}

In recent years, significant advances on three fronts have driven the implementation of QDs in *in vitro* labeling/imaging applications: (1) new QD capping ligands for rendering the nanocrystals colloidally stable in biological media, (2) bioconjugation chemistries for the attachment of biomolecules to the QD surface, and (3) methods for facilitated QD delivery to cells, reviewed in refs 5 and 15–17. To date, the most popular QDs for biological applications are still based on CdSe

Received: April 16, 2013

Revised: July 21, 2013

Published: July 23, 2013

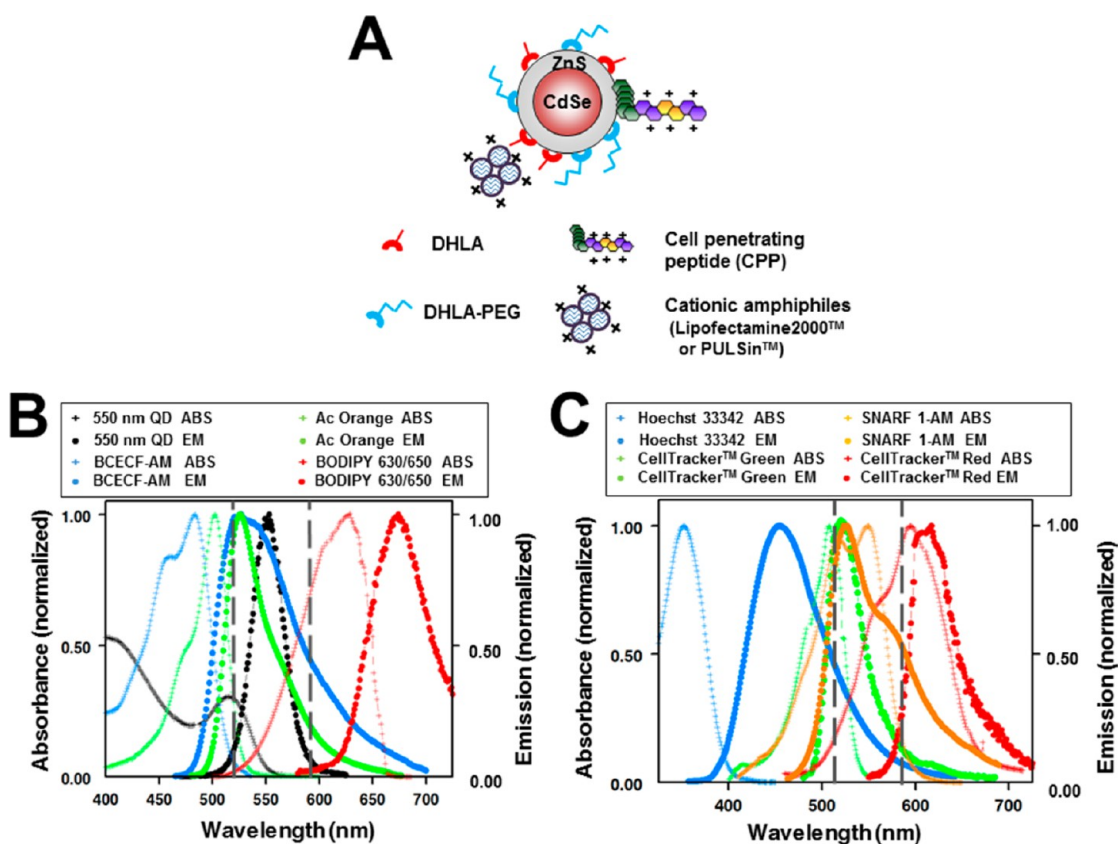


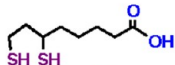
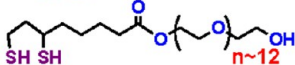
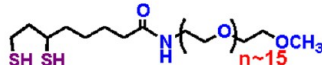
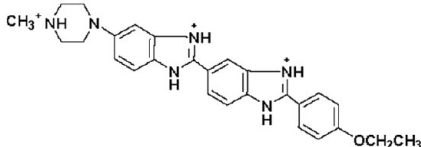
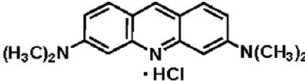
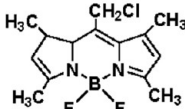
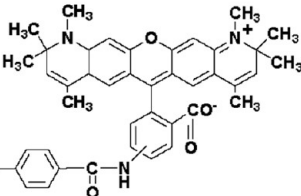

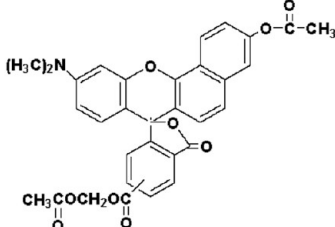
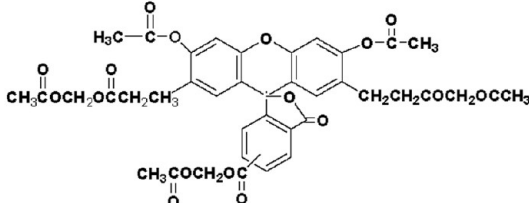
Figure 1. QD schematic and spectral properties of materials used in this study. (A) Schematic of QDs used for facilitated cellular QD delivery. CdSe/ZnS (core/shell) QDs are capped with either charged DHLA ligands or neutral DHLA-PEG ligands terminating with hydroxy or methoxy groups (structures shown in Table 1). For cellular delivery, the QDs are noncovalently associated with commercial cationic amphiphiles or histidine-appended cell penetrating peptides (CPP). (B, C) Spectra of materials used in this study. Shown are the absorption and emission spectra of 550 nm-emitting QDs and the various cell-labeling fluorophores investigated herein. The vertical dashed lines at 530 and 590 nm represent the two absorbance wavelengths of the formazan product (reduced MTS cell proliferation reagent) used to assess cellular viability (described in Materials and Methods). The absorption spectrum of the MTS/formazan product is provided in the SI (ABS, absorbance; EM, emission).

core materials as these represent the highest quality materials offering the most control over nanocrystal spectroscopic properties. Despite numerous demonstrations of relatively nontoxic cellular QD delivery, concerns regarding the cytotoxicity of released cadmium ions and the associated oxidative stress remain.^{18–23} While these concerns are valid, studies have pointed to the important role played by the QD shell and capping ligand/surface coating in mitigating the potential cytotoxicity of Cd²⁺-containing QDs within long-term cell culture.^{22,24–31} For example, Cho et al. showed that in MCF-7 cells incubated with QDs capped with mercaptopyropionic acid, CdTe core only QDs released measurable levels of free Cd²⁺ ions, while in cells incubated with CdSe core/shell QDs coated with a ZnS outer layer, intracellular Cd²⁺ levels were maintained well below the level of detection.²² Further, studies by Ryman-Rasmussen et al.²⁹ and Hoshino et al.^{31,32} have shown the contribution of both carboxylic acid and amine functions, respectively, in eliciting *in vitro* toxicity. Indeed, in our previous work, the use of poly(ethylene glycol) (PEG)-based ligands^{8,24,33} and smaller zwitterionic ligands³⁴ facilitated the realization of QD materials that manifest minimal cytotoxicity in a variety of cellular labeling/imaging applications. Clearly, the important role of overcoating shells and capping ligands in modulating the potential *in vitro* cytotoxicity of QD materials is now well-established.³⁵ Beyond cytotoxicity itself, some detailed studies have also focused on the changes in

cellular function (i.e., gene expression) that result from QD exposure.^{36,37}

It is now accepted that to be relevant and meaningful, NP toxicity testing should at a minimum: (1) utilize well-defined/characterized materials; (2) explore a relevant range of material concentrations that would be experimentally useful; and (3) examine pertinent variables such as cellular exposure time.^{38,39} Concerted efforts in this direction are now beginning to appear.^{18,36} One aspect of QDs that has been largely overlooked is the assessment of QD-associated cytotoxicity in comparison to that of traditional organic cell labeling fluorescent probes that are commonly applied for live cell labeling and imaging. The latter are generally accepted for all manners of cellular imaging with the key determinant typically consisting of not perturbing the actual experiment itself.⁴⁰ Side by side comparisons between QDs and fluorescent probes for cellular imaging have focused almost exclusively on the relative photophysical properties of each material.¹⁴ Indeed, reports on the *in vitro* cellular toxicity of organic fluorophores themselves are limited. For example, in a comprehensive 2009 review, Alford et al. performed an exhaustive search of 26 biomedical and chemical literature databases and found that while significant toxicity data was available for the US Food and Drug Administration (USFDA)-approved *in vivo* imaging dyes indocyanine green and fluorescein, surprisingly little information on many non USFDA-approved fluorophores was

Table 1. Select Properties of the Materials Utilized in This Study

Material	Structure	Mw / net charge pH 7.4	Refs
QD ligands:			
DHLA		208 / negative	[46]
DHLA-PEG-OH		~781 / neutral	[24]
DHLA-PEG-OCH ₃		~926 / neutral	[24]
Cell penetrating peptide (CPP)	R ₉ GGLA(Aib)SGWKH ₆	3200 / +10.5	[33,43]
Hoechst 33342		616 / +1	[48]
Acridine orange		301.8 / +1	[49]
CellTracker™ Green BODIPY		296.6 / 0	[50]
CellTracker™ Red CMTPX		686.3 / 0	[50]
BODIPY 630/650 methyl bromide		449.1 / 0	[56]
SNARF 1-AM		567.6 / 0	[56]
BCECF		820.7 / 0	[56]

available.⁴¹ To the best of our knowledge, limited to no attempts have been made to perform a direct, comparative analysis of the *in vitro* toxicities of QDs and organic

fluorophores. Such studies are clearly warranted to put QDs into the context of these more traditional cell labeling materials with respect to their effects on cellular proliferation during

labeling and imaging. We note that the *in vivo* toxicity of QDs in animal models is a far more complex subject and is not our focus here.^{31,42}

In this report, we conduct a comprehensive comparative study of the *in vitro* cellular cytotoxicity of our in-house synthesized CdSe/ZnS core/shell materials. Compared to commercial QD preparations in which the surface character cannot be controlled or is not known due to proprietary concerns, the use of our in-house materials allowed us to directly assess the effect of the QD surface ligand on cellular toxicity. While varying the structure of the surface capping ligand, we assessed the effect of our QD materials on the cellular proliferation of a number of cell lines of different morphological lineages when the materials were delivered *via* several different facilitated delivery modalities. Our results demonstrate that QD-associated cytotoxicity, when observed, is a function of a number of factors including: QD ligand structure, QD dose (concentration and time of incubation during delivery), and the method of facilitated QD delivery. Further, we note differences in the degree of cytotoxicity among the various cell lines tested. Finally, we show that a number of commercially available cell labeling fluorophores utilized primarily for live cell imaging and tracking elicit varying inhibitory effects on cellular proliferation within the concentration range required for efficient labeling. Cumulatively, our results place these QD materials within the context of more traditionally used fluorophores for cellular labeling and demonstrate that these QD materials can function as a relatively nontoxic alternative to cell labeling fluorophore probes under appropriate incubation and delivery conditions within cell culture systems.

RESULTS

Rationale, Selection of Materials, and Assay Format.

Our goals in this study were twofold. First, we examined the role played by the QD surface capping ligand coupled with the QD dose and mode of QD delivery in mediating QD-induced cytotoxicity. For this, QDs were exposed to cells in their native state or in conjunction with facilitated uptake modalities; these relied on conjugation to cell penetrating peptides (CPPs) and the use of cationic amphiphile complexes such as Lipofectamine 2000 and PULSin. The second goal was to compare the above effects to traditional cell-permeable fluorescent dyes when applied for similar cellular labeling utility. Specifically, we focused on the relevant concentration ranges over which each of these respective materials achieve efficient labeling of cells and cellular structures (endosomes and cytosol for QDs and cytosol and nuclei for dyes) and we determine their corresponding effects on cellular proliferation. As our previous studies have demonstrated the cumulative role played by delivery modality, concentration, and incubation time in determining overall toxicity,³³ care was taken in this study to determine cellular toxicity at comparable levels of uptake of the respective materials.

In this study we employed our in-house synthesized CdSe/ZnS core/shell QDs as a prototypical platform (Figure 1a). In previous studies, we have demonstrated the utility of these materials in a variety of cellular applications including the two-color labeling of endocytic vesicles,⁴³ the delivery of QD-appended cargos,⁴⁴ the simultaneous multicolor labeling of cellular structures using innate cellular uptake processes/interactions,⁸ and the real-time sensing of cytosolic pH.⁴⁵ We have further employed these same QD materials as a platform

for the identification of multifunctional, multidomain peptidyl motifs for the efficient endocytic uptake, and endosomal escape of materials to the cellular cytosol.³³ Importantly, throughout these aforementioned targeted investigations, we observed minimal perturbation of cellular proliferation over the dose range (QD concentration and incubation time) utilized. As shown in Table 1, three varieties of dihydrolipoic acid (DHLLA)-ligands were employed. DHLLA, the shortest of the ligand species, terminates in a carboxyl group which has to be maintained in a charged state to mediate the colloidal stability of the QD.^{43,46} Two DHLLA-appended ligands containing PEG were also queried; here, the PEG mediates colloidal stability in contrast to charge. These ligands, referred to as DHLLA-PEG-OH and DHLLA-PEG-OCH₃, terminate in hydroxy and methoxy functional groups, respectively. The DHLLA-PEG-OH has ~12 ethylene oxide repeats (M_w ~600) while the DHLLA-PEG-OCH₃ has ~15 (M_w ~750). In previous studies, these ligands have been shown to be relatively nonfouling and to mediate superior QD colloidal stability over wide pH ranges.²⁴ It was noted in those studies, however, that during the synthesis of the hydroxyl terminated DHLLA-PEG-OH ligand, the reduction step necessary for ring-opening to yield the bidentate thiol anchoring group could decompose the ester linkage.^{24,47} Further, the labile ester linkage could prove susceptible to hydrolysis in cellular environments. Indeed, these very issues spurred the development of non-ester-containing DHLLA-PEG ligands that terminated in a methoxyl group.^{24,47}

For comparison to traditional fluorophores, we selected a panel of seven cell-labeling fluorophores that have been used widely in cell biological applications. While these probes all share the common characteristic of being cell-permeant, they differ in their structures (see Table 1), spectral properties and mechanisms of action/cellular labeling. A comparison of the spectra of these fluorophores and the QDs used in this study are shown in Figure 1b,c and their relevant photophysical properties are listed in Table S1. Among the probes selected for analysis were the nucleic acid-labeling fluorophores Hoechst 33342 and acridine orange which interact with DNA *via* minor groove binding⁴⁸ and intercalation,⁴⁹ respectively. The CellTracker Green BODIPY and CellTracker Red CMTPX probes contain a chloromethyl group that reacts with thiol groups, presumably located on glutathione, which is present in the cytosol at concentrations of ~10 mM.⁵⁰ The resulting fluorophore–glutathione adducts become cell-impermeant and are retained within living cells through several generations, partitioning among daughter cells during cell division. Accordingly, they have been used as tools for the long-term visualization of cells in culture⁵¹ and for the assessment of cell viability.⁵² The BODIPY 630/650 methyl bromide fluorophore has been used to visualize host cell–pathogen interactions^{53,54} while the SNARF 1 AM and BCECF-AM probes are widely employed as pH indicator dyes due to their pH-dependent emission spectra.^{55,56}

The general assay format experimentally utilized here first exposed a range of material (QDs, QD-complexes or dyes) to target cells for 1, 4, or 24 h followed by cell proliferation for 72 h and finished with an assessment of cellular proliferation in comparison to unexposed control cells. In the second part of the assay, we determined the minimal concentration to achieve efficient cellular labeling; this is defined as the labeling of a minimum of 80% of cells quantified over multiple fields of view in separate experiments. Lastly, we determine the correspond-

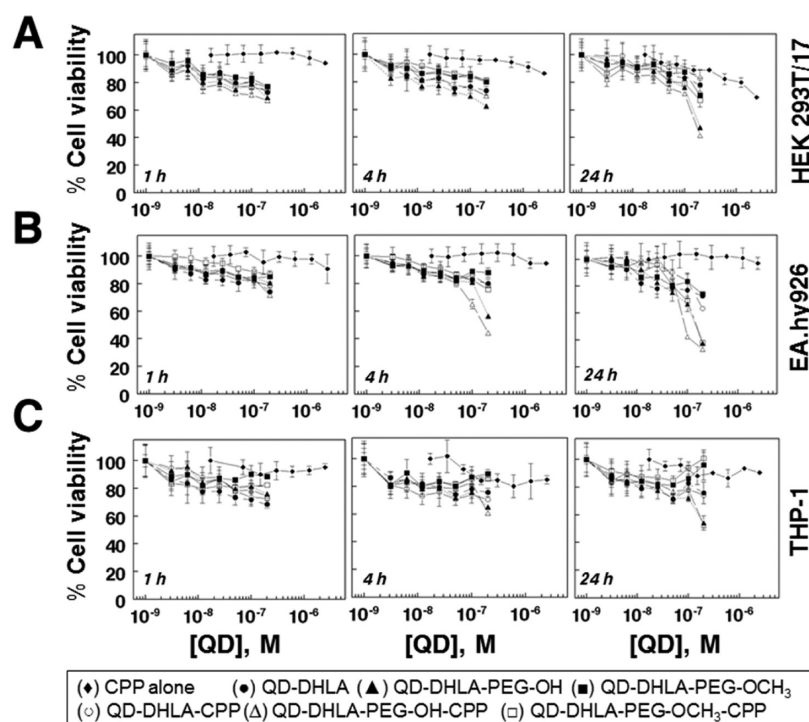


Figure 2. Representative MTS cellular proliferation assay results. Shown are the results of proliferation assays for the time-dependent CPP-mediated cellular delivery of 550 nm QDs to HEK 293T/17 (panel A), EA.hy926 (panel B), and THP-1 (panel C) cells. CPP alone, QDs alone, or QD-CPP complexes were incubated with cells for the times indicated followed by washing and a 72 h proliferation period and assessment of cellular viability by MTS assay. Each data point represents the mean \pm standard deviation (SD) of wells performed in quadruplicate.

Table 2. Cytotoxicity of QDs and QD-CPP Complexes

Exposure Time	Cellular viability (%) ^a or IC ₅₀ ^b ([QD], M)		
	1 h	4 h	24 h
QDs alone			
HEK293T/17 cells			
DHLA	78 \pm 2%	76 \pm 3%	78 \pm 5%
DHLA-PEG-OH	76 \pm 1.0%	62 \pm 1%	3 \pm 1 \times 10 ⁻⁷
DHLA-PEG-OCH ₃	81 \pm 4%	82 \pm 2%	71 \pm 1%
EA.hy926 cells			
DHLA	74 \pm 2%	80 \pm 3%	73 \pm 3%
DHLA-PEG-OH	81 \pm 4%	4 \pm 1 \times 10 ⁻⁷	2 \pm 1 \times 10 ⁻⁷
DHLA-PEG-OCH ₃	85 \pm 4%	88 \pm 3%	74 \pm 2%
THP-1 cells			
DHLA	69 \pm 3%	76 \pm 3%	76 \pm 8%
DHLA-PEG-OH	76 \pm 2%	65 \pm 2%	4 \pm 1 \times 10 ⁻⁷
DHLA-PEG-OCH ₃	89 \pm 2%	89 \pm 3%	97 \pm 9%
QD-CPP complexes			
HEK293T/17 cells			
CPP alone	94 \pm 1%	86 \pm 1%	69 \pm 2%
DHLA	76 \pm 1%	81 \pm 2%	83 \pm 6%
DHLA-PEG-OH	67 \pm 2%	70 \pm 2%	3 \pm 1 \times 10 ⁻⁷
DHLA-PEG-OCH ₃	80 \pm 1%	81 \pm 2%	67 \pm 5%
EA.hy926 cells			
CPP alone	90 \pm 11%	95 \pm 3%	96 \pm 6%
DHLA	79 \pm 3%	79 \pm 1%	64 \pm 2%
DHLA-PEG-OH	72 \pm 3%	3 \pm 1 \times 10 ⁻⁷	2 \pm 1 \times 10 ⁻⁷
DHLA-PEG-OCH ₃	87 \pm 2%	76 \pm 3%	2 \pm 1 \times 10 ⁻⁷
THP-1 cells			
CPP alone	95 \pm 3%	92 \pm 3%	92 \pm 2%
DHLA	73 \pm 2%	71 \pm 3%	74 \pm 2%
DHLA-PEG-OH	75 \pm 1%	61 \pm 1%	4 \pm 1 \times 10 ⁻⁷
DHLA-PEG-OCH ₃	82 \pm 2%	85 \pm 2%	98 \pm 4%

^aCellular viability assessed by MTS assay 72 h after initial incubation with material. The % viability shown in blue corresponds to the highest concentration tested (200 nM QD alone, 5 μ M CPP alone, or 200 nM QD/5 μ M CPP complex). ^bIC₅₀ values are in red and were determined by a fit of the data to a three-parameter curvefit function.

ing cellular viability at this effective concentration. To determine cellular viability, MTS cell proliferation or cytotoxicity assays were performed in three cell lines

representing distinct cellular lineages/morphologies; human embryonic kidney cells (HEK 293T/17 - epithelial), human umbilical vein cells (EA.hy926 - endothelial), and human acute

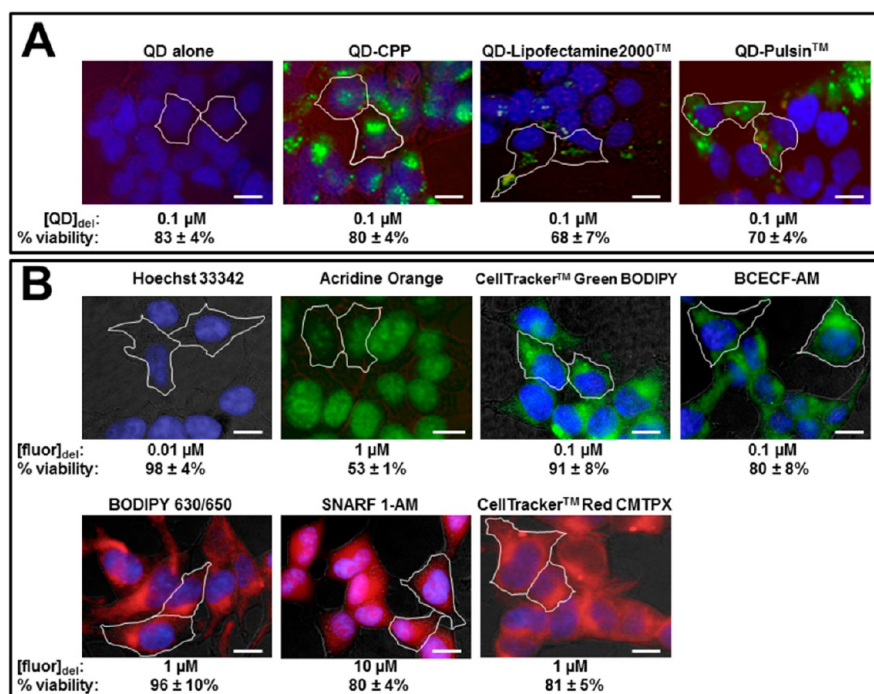


Figure 3. Comparative labeling concentrations and cytotoxicities for QDs and cell labeling fluorophore deliveries to epithelial cells. Shown are representative images of HEK 293T/17 cells labeled with 550 nm QDs capped with DHLA-PEG-OCH₃ ligands using various delivery agents (panel A) or cell labeling fluorophores (panel B). Panels show the fluorescence corresponding to QD or fluorophore merged with DAPI (nuclei) and DIC (except for the nuclear fluorophores Hoechst 33342 and acridine orange). Individual cells are outlined in white for clarity. For each image, the concentration required to achieve a labeling efficiency of at least 80% is given ([QD]_{del} or [fluor]_{del}) along with the percent cellular viability corresponding to that concentration. Scale bar is 50 μm. For all deliveries a 1 h incubation time was used except for Lipofectamine2000- or PULSIn-mediated QD delivery wherein a 4 h incubation time was used. Note that negligible cellular uptake was observed for QDs alone.

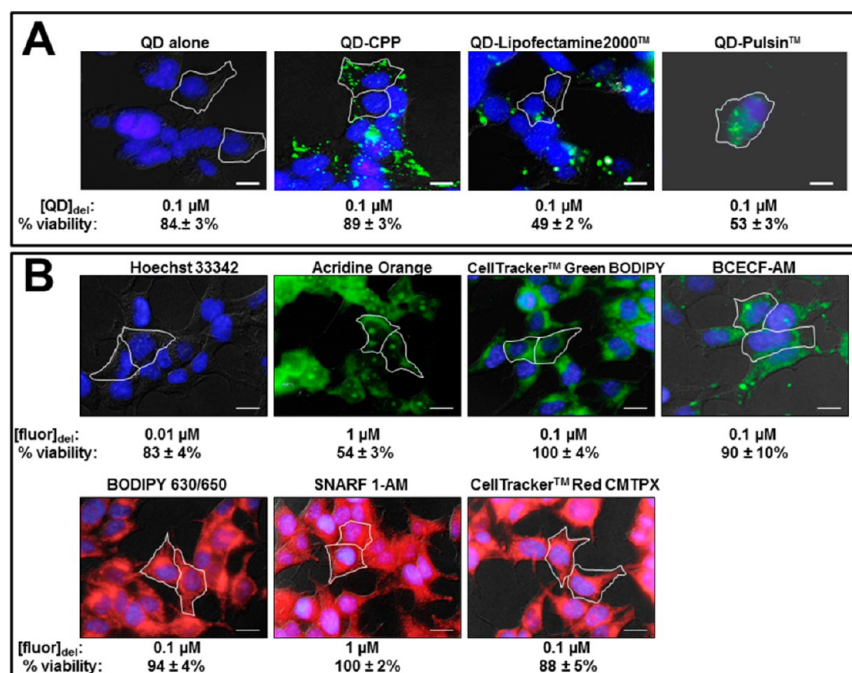


Figure 4. Comparative labeling concentrations and cytotoxicities for QDs and cell labeling fluorophore deliveries to endothelial cells. Shown are representative images of EA.hy926 endothelial cells labeled with 550 nm QDs capped with DHLA-PEG-OCH₃ ligands using various delivery agents (panel A) or cell labeling fluorophores (panel B). Panels show the fluorescence corresponding to QD or fluorophore merged with DAPI (nuclei) and DIC (except for the nuclear fluorophores Hoechst 33342 and acridine orange). Individual cells are outlined in white for clarity. For each image, the concentration required to achieve a labeling efficiency of at least 80% is given ([QD]_{del} or [fluor]_{del}) along with the percent cellular viability corresponding to that concentration. Scale bar is 50 μm. For all deliveries a 1 h incubation time was used except for Lipofectamine2000- or PULSIn-mediated QD delivery wherein a 4 h incubation time was used. Note that negligible cellular uptake was observed for QDs alone.

Table 3. Cytotoxicity of QD-Cationic Amphiphile Complexes

Exposure Time	Cellular viability (%) ^a or IC ₅₀ ^b ([QD], M)		
	1 h	4 h	24 h
QD-Lipofectamine 2000TM complexes			
HEK293T/17 cells			
Lipofectamine 2000 TM alone	73 ± 2%	81 ± 4%	60 ± 2%
DHLA	3 ± 1 × 10 ⁻⁷	2 ± 1 × 10 ⁻⁷	8 ± 2 × 10 ⁻⁹
DHLA-PEG-OH	2 ± 1 × 10 ⁻⁷	2 ± 1 × 10 ⁻⁷	3 ± 1 × 10 ⁻⁹
DHLA-PEG-OCH ₃	2 ± 1 × 10 ⁻⁷	2 ± 1 × 10 ⁻⁷	2 ± 1 × 10 ⁻⁹
EA.hy926 cells			
Lipofectamine 2000 TM alone	70 ± 5%	70 ± 2%	64 ± 1.5%
DHLA	1 ± 0 × 10 ⁻⁷	6 ± 2 × 10 ⁻⁸	9 ± 2 × 10 ⁻⁹
DHLA-PEG-OH	4 ± 1 × 10 ⁻⁸	4 ± 1 × 10 ⁻⁸	4 ± 1 × 10 ⁻⁹
DHLA-PEG-OCH ₃	5 ± 1 × 10 ⁻⁸	4 ± 1 × 10 ⁻⁸	2 ± 1 × 10 ⁻⁹
THP-1 cells			
Lipofectamine 2000 TM alone	75 ± 3%	58 ± 2%	1 ± 0 × 10 ⁻⁹
DHLA	54 ± 4%	60 ± 4%	59 ± 6%
DHLA-PEG-OH	73 ± 4%	64 ± 9%	55 ± 3%
DHLA-PEG-OCH ₃	78 ± 4%	83 ± 2%	63 ± 3%
QD-PULSinTM complexes			
HEK293T/17 cells			
PULSin TM alone	93 ± 4%	70 ± 2%	75 ± 5%
DHLA	65 ± 2%	65 ± 1%	71 ± 1%
DHLA-PEG-OH	72 ± 4%	79 ± 2%	79 ± 1%
DHLA-PEG-OCH ₃	77 ± 6%	66 ± 7%	69 ± 2%
EA.hy926 cells			
PULSin TM alone	88 ± 3%	92 ± 4%	65 ± 3.4%
DHLA	60 ± 1%	2 ± 1 × 10 ⁻⁷	1 ± 0 × 10 ⁻⁸
DHLA-PEG-OH	3 ± 0 × 10 ⁻⁷	1 ± 0 × 10 ⁻⁷	9 ± 0 × 10 ⁻⁹
DHLA-PEG-OCH ₃	3 ± 1 × 10 ⁻⁷	2 ± 1 × 10 ⁻⁷	1 ± 0 × 10 ⁻⁸
THP-1 cells			
PULSin TM alone	85 ± 2%	76 ± 1%	61 ± 5%
DHLA	84 ± 7%	70 ± 3%	68 ± 5%
DHLA-PEG-OH	76 ± 2%	67 ± 7%	73 ± 8%
DHLA-PEG-OCH ₃	83 ± 3%	73 ± 4%	79 ± 3%

^aCellular viability assessed by MTS assay 72 h after initial incubation with material. The % viability shown in blue corresponds to the highest concentration tested (200 nM QD-cationic amphiphile complex or equivalent amount of amphiphile alone). ^bIC₅₀ values are in red and were determined by a fit of the data to a three-parameter curvefit function.

monocytic leukemia (THP-1 - monocytic). See Methods section for full description. This quantitative assay format has been widely used to assess the effects of a myriad of materials on cellular proliferation, including QDs^{33,57–61} and cell labeling dyes.⁴¹

Cytotoxicity of the QDs and QD-CPP Complexes. We began by analyzing the cytotoxicity of 550 nm emitting QDs when incubated alone or as a complex with various agents for their facilitated delivery using CPPs or cationic amphiphiles (see below). The CPPs were ratiometrically self-assembled to the QDs using metal-affinity coordination driven by the peptides terminal His₆ sequence. This assembly process just requires mixing of the QD with peptide at a desired molar ratio, occurs nearly spontaneously, and allows for control over the number of peptides conjugated per QD.⁶² Previous studies have shown that the current QDs can be controllably assembled to a maximum of ~50 ± 10 peptides.⁶³

Experiments revealed general trends with regards to the role played by the QD capping ligand, delivery vehicle, and incubation time. Figure 2 shows representative cellular proliferation assay data for the cell lines investigated here (for both QDs alone and QD-CPP complexes) as a function of QD concentration, incubation time, and surface capping ligand. The corresponding cytotoxicity results including percent cellular viability at the highest exposure concentration and IC₅₀ (half maximal inhibitory concentration) values when reached are summarized in Table 2. Incubation of cells with QDs alone proved largely innocuous with almost no uptake noted at incubation times of 1 h and demonstrated cellular viabilities of nearly 75% or greater noted for the different capping ligands

across all cell lines for the highest QD concentration tested (200 nM) except for THP-1 monocytic cells in the presence of DHLA-QDs; viability 68.5%. Indeed, these viabilities correlate well with the minimal nonspecific binding observed for these materials (Figure 3a and Figure 4a) and confirm our previous findings.^{33,43} Interestingly, DHLA-PEG-OH was the only capping ligand that elicited significant and consistent toxicity, with inhibition of proliferation of all three cell lines first apparent at 4 h incubation and reaching a maximum upon 24 h incubation. Here, IC₅₀ values of 210–400 nM were noted across all three cell lines tested, suggesting the susceptibility of the labile ester linkage to extracellular esterases^{64,65} leading to the formation of poly(glycolic acid) and other adducts such as aldehydes; these have been reported to inhibit cellular proliferation in multiple cell lines *in vitro*, as reviewed in ref 66.

The use of peptides for the cellular uptake of QDs and other nanoparticle (NP) materials has been established as one of the most popular and effective delivery modalities given the peptides' small size, ease of synthesis, and advancements in NP-peptide bioconjugation chemistries.^{17,67,68} Here, when incubated with cells for 1 h as a complex with a nine-arginine containing CPP self-assembled *via* His₆-metal coordination to the QD surface at a ratio of 25 CPP/QD, efficient cellular uptake of all QDs was noted at 100 nM QD. Again, efficient cellular labeling was defined as the labeling of a minimum of 80% of cells quantified over separate experiments. As shown in Figure 3a the QDs adopted a perinuclear morphology consistent with QD endocytosis and sequestration as has been reported previously for peptides of this nature.^{3,4,43} Similarly, efficient uptake was observed in EA.hy926 cells at 100

Table 4. Cytotoxicity of Selected Cell Labeling Fluorophores

Exposure Time	Cellular viability ^a (%) or IC ₅₀ ^b ([probe], M)		
	1 h	4 h	24 h
Hoechst 33342 (10 ⁻⁷ -10 ⁻⁶ M)			
HEK293T/17 cells	5 ± 1 x 10 ⁻⁶	6 ± 2 x 10 ⁻⁶	5 ± 1 x 10 ⁻⁷
EA.hy926 cells	9 ± 3 x 10 ⁻⁶	3 ± 1 x 10 ⁻⁶	6 ± 2 x 10 ⁻⁷
THP-1 cells	72 ± 8%	70 ± 3%	65 ± 2%
Acridine orange (10 ⁻⁶ M)			
HEK293T/17 cells	4 ± 1 x 10 ⁻⁶	4 ± 1 x 10 ⁻⁶	9 ± 3 x 10 ⁻⁷
EA.hy926 cells	4 ± 1 x 10 ⁻⁶	6 ± 1 x 10 ⁻⁶	8 ± 2 x 10 ⁻⁷
THP-1 cells	82 ± 2%	81 ± 5%	79 ± 3%
CellTracker™ Green BODIPY (10 ⁻⁷ -10 ⁻⁵ M)			
HEK293T/17 cells	1 ± 0 x 10 ⁻⁴	2 ± 1 x 10 ⁻⁴	2 ± 1 x 10 ⁻⁴
EA.hy926 cells	100 ± 6%	86 ± 3%	2 ± 0 x 10 ⁻⁴
THP-1 cells	81 ± 4%	80 ± 1%	82 ± 2%
CellTracker™ Red CMTPX (10 ⁻⁷ -10 ⁻⁵ M)			
HEK293T/17 cells	68 ± 2%	65 ± 1%	1 ± 0 x 10 ⁻⁵
EA.hy926 cells	70 ± 2%	78 ± 3%	7 ± 1 x 10 ⁻⁶
THP-1 cells	72 ± 3%	60 ± 2%	56 ± 2%
BODIPY 630/650 (10 ⁻⁷ -10 ⁻⁵ M)			
HEK293T/17 cells	5 ± 1 x 10 ⁻⁵	7 ± 2 x 10 ⁻⁶	5 ± 2 x 10 ⁻⁶
EA.hy926 cells	6 ± 2 x 10 ⁻⁵	7 ± 1 x 10 ⁻⁶	4 ± 1 x 10 ⁻⁶
THP-1 cells	8 ± 2 x 10 ⁻⁵	10 ± 1 x 10 ⁻⁶	5 ± 2 x 10 ⁻⁶
SNARF 1-AM (10 ⁻⁶ -10 ⁻⁵ M)			
HEK293T/17 cells	80 ± 5%	64 ± 4%	61 ± 7%
EA.hy926 cells	101 ± 7%	101 ± 7%	87 ± 9%
THP-1 cells	67 ± 1%	68 ± 2%	70 ± 3%
BCECF-AM (10 ⁻⁷ -10 ⁻⁶ M)			
HEK293T/17 cells	5 ± 2 x 10 ⁻⁶	9 ± 2 x 10 ⁻⁷	4 ± 1 x 10 ⁻⁷
EA.hy926 cells	3 ± 1 x 10 ⁻⁶	1 ± 0 x 10 ⁻⁶	1 ± 0 x 10 ⁻⁶
THP-1 cells	6 ± 2 x 10 ⁻⁵	5 ± 2 x 10 ⁻⁵	4 ± 2 x 10 ⁻⁵

^aCellular viability assessed by MTS assay 72 h after initial incubation with material. The % viability shown in blue corresponds to the highest concentration tested. Manufacturer's suggested working concentration for each fluorophore is in parentheses. ^bIC₅₀ values are in red and were determined by a fit of the data to a three-parameter curvefit function.

nM QD (Figure 4a). Not only did this dosing regime (100 nM QD/1 h incubation) result in robust cellular labeling, it was coupled with cellular viabilities reflecting that under these delivery conditions the materials were well tolerated across multiple cell lines. Of particular note was the viability exhibited by CPP complexes of DHLA-PEG-OCH₃-capped QDs where viabilities of nearly 80% or greater were noted in all three cell lines tested. Increasing the incubation time to 4 h did not negatively impact cellular viability. This result is notable, particularly within the context of the cellular delivery of QDs bearing mixed peptide surfaces (e.g., where one peptide mediates cellular uptake while a second directs localization to subcellular organelles/structures⁶⁹ or serves a sensing function). In these instances, longer incubation times are often required to facilitate optimal localization or sustained sensing, and our results indeed suggest that our QD materials are well-tolerated over this operational window. The only ligand species that manifested an appreciable degree of cytotoxicity when delivered as a CPP complex was again the DHLA-PEG-OH ligand. Here, we were able to measure IC₅₀ values of ~400 nM in EA.hy926 endothelial cells (incubation time of 4 h) while IC₅₀ values of 150–400 nM QD were observed in all three cell lines when the incubation time was increased to 24 h. No significant deleterious effect on viability was noted for the CPP alone regardless of cell line or incubation time used.

Cytotoxicity of the QD-Amphiphile Complexes.

Cationic amphiphiles are quite commonly employed for the efficient delivery of QDs for the purpose of *in vitro* labeling and imaging.^{15,33,70,71} Here, we analyzed the cytotoxicity of QDs when delivered to cells using two commercial cationic amphiphile preparations: Lipofectamine 2000 (LF2000) and PULSin. LF2000 consists of a proprietary cationic liposome formulation containing a neutral colipid which is believed to complex with (negatively charged) molecules to aid them in

overcoming electrostatic repulsion at the cell membrane. PULSin is a proprietary amphiphilic polymer originally designed as a cytosolic delivery agent for proteins. In contrast to CPP-mediated QD delivery, the use of amphiphiles requires longer incubation regimes (typically on the order of 3–4 h) to achieve effective cellular QD uptake at 100 nM QD.^{33,70} LF2000 has been shown to deliver QDs to endosomes³³ as well as to the cellular cytosol⁷⁰ and we have previously shown that PULSin mediates the partial escape of endocytosed QDs to the cytosol, although this process requires 4–5 days after initial delivery and is coupled with a moderate degree of cytotoxicity that is largely attributable to the added presence of the PULSin delivery agent in the complex.³³ For assays with the cationic amphiphiles, QDs were mixed with materials at the concentrations and times indicated prior to cellular exposure (see the Methods section).

In the current study, these agents alone exhibited clear cell line-dependent effects on cellular proliferation for the 4 h delivery incubation time, exhibiting viabilities that ranged from 57% (THP-1) to 80% (HEK 293T/17) for LF2000 or 70% (HEK 293T/17) to 92% (EA.hy926) for PULSin. Cellular viability data are summarized and presented in Table 3 (see also Figures S2 and S3 for cell proliferation plots for LF2000 and PULSin, respectively). Focusing on the 4 h incubation window (the time frame required for efficient QD-amphiphile labeling of 80% of cells), LF2000-QD-DHLA-PEG-OCH₃ complexes efficiently labeled the endosomal compartments of HEK 293T/17 cells when delivered at 100 nM and this was coupled with a viability of 68% (Figure 3a). These same complexes also effectively labeled EA.hy926 cells, although the viability was significantly reduced to 49% (Figure 4a). Comparable viabilities were obtained for LF2000-delivered DHLA and DHLA-PEG-OH capped QDs over the time course of this incubation regime while extending the incubation time to 24 h exacerbated effects

on cellular proliferation in both cell lines. Notably, these complexes were less impactful to THP-1 cells and in the case of the DHLA-PEG-OCH₃ ligand a modest degree of induction of cellular proliferation was observed. Similar observations have been noted, for example, in Caco-2 epithelial adenocarcinoma cells incubated with low nM concentrations of CdS QDs coated with maltodextrin.⁷² Cell line- and ligand-dependent effects on cytotoxicity were observed for PULSin-delivered QDs. As shown in Figure 3a, delivery of 100 nM QD (DHLA-PEG-OCH₃ capped) resulted in QD delivery to the cytosol coupled with 70% viability in HEK 293T/17 cells. Comparable viability results were noted for the other two ligands and for THP-1 cells.

These results reflect several key points regarding the cytotoxicity associated with facilitated delivery of QDs. Clearly, cytotoxicity, when observed, is a cumulative function of QD dose, capping ligand, delivery vehicle, and the cell line used. Further, it appears that these variables must be iteratively optimized to determine the conditions required to strike a balance between efficient labeling and concomitant cytotoxicity. Taken in this context, it is clear that, for the QDs under study here, the CPP-mediated delivery that is shown affords an optimal balance of efficient cellular QD labeling coupled with short incubation time regimes while mitigating inhibitory effects on cellular proliferation across multiple cell lines. QDs complexed with cationic amphiphiles, while efficient labeling tools, are coupled with increased cytotoxicity and require longer initial incubation times and subsequent culture times to mediate their effects.

Cytotoxicity of Selected Cell Labeling Fluorophores.

Using the same approach as that for the assessment of QD cytotoxicity (1, 4, and 24 h cellular exposure of a range of dye concentrations), we used proliferation assays to determine the incubation time-dependent cytotoxicity associated with cellular labeling using the selected panel of seven cell-permeant fluorophore probes. Table 4 summarizes the cellular viability results of these commercial cell-labeling probes assayed at the manufacturer's suggested working concentration range for cellular labeling (see Figure S4 for cell proliferation assay data plots). Examination of the data for 1 h incubation demonstrates that across multiple cell lines the majority of dyes except the CellTracker Red and SNARF 1 exhibited measurable IC₅₀ values that were within the manufacturer's recommended concentration range for cellular labeling. The CellTracker Green BODIPY only elicited toxicity in the HEK cells while the Hoechst 33342 and acridine orange DNA stains affected HEK and EA.hy926 cells. It is worth noting that the THP-1 cells showed minimal susceptibility to the antiproliferative effects of most of the fluorescent probes, with the exception of BODIPY 630/650 and BCECF for which IC₅₀ values of 84 and 61 μM were obtained at a 1 h incubation time.

An empirical titration of each fluorophore was again performed to ascertain the minimal concentration required for effective labeling of our test cell lines (80% of cells, data not shown). As shown in Figure 3b, at the concentration determined for efficient labeling, nearly all of the probes displayed >80% viabilities in HEK 293T/17 cells (except acridine orange – see below) showing that the dyes were well tolerated under these delivery conditions. Similar results were obtained for the fluorophore labeling of EA.hy926 cells (Figure 4b). Interestingly, the minor groove binding probe Hoechst 33342 elicited no deleterious effects on the proliferation of any of the cell lines tested at the 0.01 μM exposure concentration.

The one fluorophore that did exhibit considerable cytotoxicity was the DNA intercalator acridine orange. At an 80% efficient labeling concentration of 1 μM, this probe inhibited the proliferation of both HEK 293T/17 and EA.hy926 cells by ~50% upon 1 h incubation. This result, coupled with previous reports showing acridine orange to inhibit mitosis⁷³ and to induce binucleation in chondrocytes,⁷⁴ reflects the cytotoxic potential of this probe. Still, it remains one of the most widely used probes for nuclear staining in fluorescence imaging⁷⁵ and flow cytometry⁷⁶ in live cells.

DISCUSSION AND CONCLUSIONS

Our first goal was to put into context the potential *in vitro* toxicity of our CdSe/ZnS QDs as a function of a number of different parameters essential to their use in cellular labeling applications. These factors include (1) the nature of the capping ligand used to promote colloidal stability and biocompatibility, (2) the delivery modality used to facilitate QD cellular internalization, and (3) the dosage (concentration and incubation time) required to achieve efficient cellular labeling. We queried these factors in three different cell lines representing various morphological lineages (epithelial, endothelial, and monocyte) to assess their cumulative role in cellular labeling. We find that for both native QDs and QD-CPP complexes assembled with nanocrystals displaying all three ligands, no significant impairment of cellular viability is noted for 1 h delivery times. The DHLA-PEG-OH materials manifest the most cytotoxicity, 7 out of 8 reported IC₅₀ values in Table 2. This is not an extraordinary finding given the labile nature of the ester group present in this ligand and its association with inhibition of cellular proliferation.^{64–66} We note that cellular exposure to LF2000 alone can inhibit cellular proliferation and that use of this amphiphilic polymer in conjunction with all three types of QDs appears to induce significant cytotoxicity (see Table 3). Interestingly, use of PULSin to deliver QDs only elicits significant cytotoxicity in EA.Hy926 cells suggesting a potential contraindication between this polymer and some aspect of endothelial cell function or metabolism. More importantly, at the minimal exposure concentrations and times needed for efficient cellular labeling of ~80% of cells, the QD-CPP (DHLA-PEG-OCH₃ ligands, 0.1 μM, 1 h) has minimal impact on viability (<20% inhibition) while QD-LF2000 or QD-PULSin complexes (DHLA-PEG-OCH₃ ligands, 0.1 μM, 4 h) are more inhibitory (~30–50% inhibition), see Figures 3 and 4.

The relatively innocuous nature of CPP-mediated QD delivery compared to cationic amphiphile-mediated uptake further substantiates the role of peptide-mediated delivery as among the most robust in terms of combined uptake and minimal toxicity.^{33,43,44,77,78} CPPs are inherently small, biocompatible, and biodegradable, and can be relatively nontoxic for particular nanoparticle delivery applications.^{68,79,80}

Use of LF2000 to facilitate cellular uptake of QDs can, however, have some toxic side effects, and this is indeed corroborated by several other reports.^{33,70,81} Use of this polymer should thus be carefully considered within the context of a given application. In contrast, use of PULSin to facilitate QD cellular uptake only elicits a significant effect on one cell line which suggests that the choice in cell line used must also be a critical experimental consideration. It is important to note that a majority of cell lines used in bionanoresearch are, for all intents and purposes, transformed cell lines. This means that they are significantly dedifferentiated and immortal, display

heterogeneous chromosome counts, and may not reflect the full function, metabolism, and susceptibility or immunity of that same cell in primary form.^{81,82} As expected, we also note general trends where more cytotoxicity is correlated with either longer incubation times or higher exposure concentrations. The results in achieving effective cellular labeling suggest that empirically determining a minimal or “acute” dosage where cells are efficiently labeled while minimizing cytotoxicity should be a first and critically important consideration for mitigating potential adverse effects on viability.

Understanding of the role played by the capping ligand in modulating QD–cell interactions continues to grow. Prominent researchers such as Nel, Chan, Dawson, Hamad-Schifferli, and others have posited (probably correctly) that it is not the nanoparticles themselves that will drive a cellular response, but rather the presentation and concentration of surface functionalizing molecules (i.e., ligands) and biologicals (mostly proteins) displayed in an outer layer on the nanoparticle called a *corona* that will be seen by the cell and elicit a response.^{84–87} Given this, use of any surface ligand that could have detrimental cellular effects, such as that seen from putative hydrolysis of the DHLA-PEG-OH ligands here, should be avoided. Although the DHLA ligands are quite small and do not manifest significant cytotoxicity, they are still hampered by solubility issues. Gratifyingly, the DHLA-PEG-OCH₃-liganded QD materials appear to be quite innocuous. In general, use of PEGylated nanoparticles may be one of the more consistently safer approaches for cellular labeling. Indeed, PEG moieties have a long history of being both safe and accepted for widely disparate biological and medical use, and many PEGylated QD materials are commercially available or easily assembled. In particular, their nonfouling properties can help mitigate many potential issues associated with opsonization.

The comparative analysis of effects on cellular proliferation between our in-house synthesized QDs and a representative set of organic dyes commonly used for cellular labeling is perhaps the most important aspect of this study. As studies of this nature do not appear to be present in the literature, we felt such an analysis was vital to place QD utility into the context of organic dyes, given the enormous popularity QDs have achieved over the past ten years in cellular labeling, imaging, and sensing.^{15,16,88,89} We found that 5 of the 7 dyes tested elicit significant effects on cellular viability using the labeling concentration range suggested and these effects are exacerbated as exposure time to the cells is increased. Interestingly, SNARF 1 which is perhaps the closest to fluorescein in structure appears to be quite innocuous with no significant effects on cellular viability in any configuration tested. Additionally, examining the concentration required for efficient labeling with the dye panel and the corresponding cellular viabilities in comparison to the QD-CPP (Figures 3 and 4) shows that almost all the dyes do not elicit a significant effect (<20% loss of viability). In this configuration, only acridine orange manifests a significant effect of ~50% loss of viability. We do qualify this result with the fact that acridine orange is a nuclear dye and that our QD labeling assays did not label the cellular nuclei. We recognize that, aside from the nuclear stains, the dyes are all cytosolic while the QD-CPP complexes are primarily located in endosomes. However, we point out that such endocytic sequestration is the principal fate of QDs taken up by almost all cells irrespective of delivery modality.^{79,90,91} Nevertheless, examining cellular viability outcomes in conjunction with the efficient labeling result suggests that when

used in an appropriate context for cellular labeling applications (i.e., proper tuning of QD dose, surface ligand, and delivery modality), QDs are comparable to most organic dyes used in the same role and can function as robust *in vitro* cell labeling reagents that exhibit minimal impact on cellular viability.

In summation, for cellular labeling applications with QDs the identification of dosing conditions required for efficient cellular labeling/imaging will be an iterative process. Our data demonstrate the cumulative role played by many factors on mediating QDs' effects on *in vitro* cellular proliferation including ligand structure, dosage, and use of CPP or amphiphile for facilitating cellular uptake. Our results also point to cell-line dependent differences and confirm the importance of the combination of empirical, iterative testing of labeling efficiency coupled with an assessment of cytotoxicity. Most importantly, across multiple cell lines, our QDs elicit *in vitro* cytotoxicities that are comparable to many commonly used cell labeling fluorophores. Clearly, the choice of using QDs for cellular labeling should not be made on preconceived notions of toxicity but rather on whether they are the appropriate fluorophore for the targeted application.

■ MATERIALS AND METHODS

Materials. DAPI (4',6-diamidino-2-phenylindole), 2-mercaptoethanol, and paraformaldehyde were purchased from Sigma Aldrich (St. Louis, MO). Lipofectamine 2000 transfection reagent, cell culture grade phosphate buffered saline (PBS), and Dulbecco's Modified Eagle's Medium containing 25 mM HEPES (4-(2-hydroxyethyl)-1-piperazineethanesulfonic acid) (DMEM-HEPES) were obtained from Invitrogen/Life Technologies, (Carlsbad, CA). PULSin transfection reagent was a product of Polyplus-transfection (New York, NY). 96-well cell culture cluster microtiter plates were obtained from Corning-Costar (Corning, NY). All other materials/reagents were obtained as noted in the text.

Quantum Dots and Capping Ligands. The QDs used in this study were CdSe/ZnS core/shell nanocrystals with emission maxima centered at 550 nm. QD synthesis was performed stepwise using the high temperature reaction of organometallic precursors (trioctylphosphine selenium (TOP:Se), cadmium acetylacetonate, diethyl zinc, and hexamethyldisilathiane) in a hot coordinating mixture of TOP/TOPO and hexadecylamine, as described previously.⁹² QDs were made hydrophilic by exchanging the native hydrophobic ligands with either DHLA (dihydrolipoic acid) or poly(ethylene glycol) (PEG)-appended DHLA (DHLA-PEG). In this study, two variants of the DHLA-PEG capping ligand were used, wherein their distal ends terminated in either a hydroxy or methoxy functional group. These ligands are referred to herein as DHLA-PEG-OH and DHLA-PEG-OCH₃, respectively, and their synthesis is described in detail in refs 24 and 25. The spectra and structures of the QD surface ligands used in this study are shown in Figure 1 and Table 1, respectively.

Cell Labeling Fluorophores. Hoechst 33342, acridine orange, CellTracker Green BODIPY, CellTracker Red CMTPX, BODIPY 630/650 methyl bromide, carboxylic acid SNARF 1-acetoxymethyl ester (SNARF 1 a.m.), and BCECF were purchased from Invitrogen (Carlsbad, CA). The relevant spectra of the cell labeling fluorophores used herein are shown in Figure 1.

Synthesis of CPP. The cell-penetrating peptide (CPP, R₆GGLA(Aib)SGWKH₆) used in this study is described in ref

33. The polyarginine tract (R_n) that mediates cellular uptake is separated from the polyhistidine tract (H_6) (for peptide self-assembly to the QD surface) by a linker domain (GGLA(Aib)-SGWK). Aib is the artificial residue alpha-amino isobutyric acid. Peptide synthesis was performed using Boc-solid phase peptide synthesis, purified by HPLC and characterized by electrospray ionization mass spectroscopy.^{43,93} The CPP was desalted, quantitated, lyophilized and stored at $-20\text{ }^\circ\text{C}$ until needed using methods similar to that described in ref 94.

Cell Lines and Cell Culture. HEK 293T/17 (epithelial), EA.hy926 (endothelial), and THP-1 (monocytic) cell lines were obtained from American Type Culture Collection (ATCC, Manassas, VA). HEK 293T/17 and EA.hy926 cells were grown as adherent monolayers in complete growth medium (Dulbecco's Modified Eagle's Medium (DMEM; purchased from ATCC)) supplemented with 1% (v/v) antibiotic/antimycotic and 10% (v/v) heat inactivated fetal bovine serum (ATCC). THP-1 cells were grown in suspension in RPMI-1640 (ATCC) containing 10% fetal bovine serum and 0.05 mM 2-mercaptoethanol. All cells were cultured in T25 flasks and incubated at $37\text{ }^\circ\text{C}$ under 5% CO_2 atmosphere in a humidified incubator. A subculture was performed every 3–4 days as described.⁴³ All cells in this study were used between passages 3 and 10.

Cellular Delivery of Quantum Dots, Quantum Dot-Delivery Agent Complexes, and Cell Labeling Fluorophores. For delivery experiments, cells were seeded in complete growth medium (typically $\sim 1 \times 10^4$ cells/well) into the wells of Lab-Tek 8-well chambered #1 borosilicate coverglass (Nalge Nunc, Rochester, NY) and cultured overnight. Prior to the addition of materials for cellular delivery, the cells were washed once with PBS. For incubation of cells with QDs alone, a stock solution of QDs was diluted into DMEM-HEPES. QD-CPP bioconjugates were formed by diluting the CPP into DMEM-HEPES followed by the addition of a stock solution of QDs to achieve a ratio of 25:1 (CPP:QD). The CPP was self-assembled onto the QD surface for 20 min prior to addition to the cells.³³ QD-Lipofectamine 2000 complexes were generated by incubation of QDs with the reagent for 20 min in DMEM-HEPES at a ratio of $1\text{ }\mu\text{L}$ Lipofectamine 2000 per 1.5 pmol QD. QD-Pulsin reagent complexes were formed by dilution of the QDs into HEPES buffer (pH 8.2) followed by addition of the transfection reagent ($1\text{ }\mu\text{L}$ reagent per pmol QD). The final assembled complexes were diluted into DMEM-HEPES then added to the cells. For labeling of cells with cell staining dyes, the as-supplied materials were diluted into DMEM-HEPES and incubated with the cells according to the manufacturer's instructions. For all materials, imaging was performed on a concentration range of delivered materials to empirically determine the minimum concentration required for robust staining, defined as the reproducible labeling of at least 80% of cells.

Microscopy and Image Analysis. The intracellular distribution of QDs was analyzed by differential interference contrast (DIC) and epifluorescence microscopy using an Olympus IX-70 total internal reflection fluorescence microscope equipped with 60 \times and 100 \times oil immersion objectives. Samples were excited using a Xe lamp and images were collected using standard filter sets for DAPI, FITC (for QDs), TRITC, and Cy5. Merged images were generated using Adobe PhotoShop. Quantification of cellular uptake of QDs and cell labeling fluorophores was performed in either PhotoShop or Image J.

Quantification of Cytotoxicity. The cytotoxicities of QDs, QD-peptide/QD-transfection reagent complexes, and cell staining dyes were assessed using the Promega CellTiter96 Aqueous One Solution cell proliferation assay. This assay is a colorimetric method for determining the number of viable cells after incubation with a material of interest. The One Solution reagent contains a novel tetrazolium compound [3-(4,5-dimethylthiazol-2-yl)-5-(3-carboxymethoxyphenyl)-2-(4-sulphophenyl)-2H-tetrazolium, inner salt; MTS] and an electron coupling reagent (phenazine ethosulfate; PES). PES has enhanced chemical stability, which allows it to be combined with MTS to form a stable solution. The MTS tetrazolium compound is bio-reduced by cells into a blue formazan product that is soluble in tissue culture medium. This conversion is accomplished primarily by NADPH or NADH produced by dehydrogenase enzymes in metabolically active (viable) cells^{95,96} and the absorbance of the resulting colored product is proportional to the number of viable cells in the well. Cells were seeded to the wells of 96-well tissue culture-treated microtiter plates at the following initial densities: HEK 293T/17 cells (doubling time (DT) per ATCC, ~ 24 h): 4000 cells/well; EA.hy926 cells (DT, ~ 31 h): 4000 cells/well; THP-1 cells (DT, 35–40 h): 5000 cells/well. These cell seeding densities were determined empirically to ensure that the resulting color formation at the assay end point was within the linear range. Various times of incubation (1, 4, and 24 h) of the materials with the cells were purposefully used to determine the effects of short- (acute), mid-, and long-term (chronic) incubation regimes on cellular proliferation. Following the incubation period on the cells, the materials were removed and the cells were washed once with fresh culture media. Following this wash and replacement with fresh media, the cells were allowed to proliferate under standard culture conditions for 72 h at which time the MTS reagent ($20\text{ }\mu\text{L}$) was added to each well and incubated for 4 h to allow sufficient color formation. The formazan product resulting from reduction of the MTS reagent absorbs over a wide range (~ 400 – 650 nm) of the visible spectrum with an absorbance maximum at 490 nm. Thus, the absorbance of each well was read at either 530 nm (for the red-absorbing fluorophores) or 590 nm (for the blue/green-absorbing fluorophores and QDs) (see Table S1 for details). When sufficient cytotoxicity was noted, IC_{50} values were determined using a three parameter curvefit function within SlideWrite analysis software (v 7.01, Advanced Graphics, Rancho Santa Fe, CA). When IC_{50} values were not reached, the percent cell viability corresponding to the highest concentration tested is reported. Data are reported as the average \pm standard deviation (SD) of wells performed in quadruplicate.

■ ASSOCIATED CONTENT

📄 Supporting Information

Additional experimental results. This material is available free of charge via the Internet at <http://pubs.acs.org>.

■ AUTHOR INFORMATION

Corresponding Author

*E-mail: james.delehanty@nrl.navy.mil; igor.medintz@nrl.navy.mil.

Present Address

Christopher Bradburne, Applied Biological Sciences Group, Asymmetric Operations Department, The Johns Hopkins

University, Applied Physics Laboratory, 11100 Johns Hopkins Road, Laurel, MD 20723–6099. Hedi Mattoussi, Department of Chemistry and Biochemistry, Florida State University, Tallahassee, FL 23306, USA.

Author Contributions

Christopher E. Bradburne and James B. Delehanty contributed equally to this work.

Notes

The authors declare no competing financial interest.

ACKNOWLEDGMENTS

The authors acknowledge the NRL NSI and Base Funding Program, DARPA, and DTRA JSTO MIPR # B112582M. CB was supported by a National Research Council (NRC) Associateship.

REFERENCES

- (1) Shaner, N. C., Steinbach, P. A., and Tsien, R. Y. (2005) A guide to choosing fluorescent proteins. *Nat. Methods* 2, 905–909.
- (2) Giepmans, B. N., Adams, S. R., Ellisman, M. H., and Tsien, R. Y. (2006) The fluorescent toolbox for assessing protein location and function. *Science* 312, 217–224.
- (3) Sawant, R., and Torchilin, V. (2010) Intracellular transduction using cell-penetrating peptides. *Mol. Biosyst.* 6, 628–640.
- (4) Fonseca, S. B., Pereira, M. P., and Kelley, S. O. (2009) Recent advances in the use of cell-penetrating peptides for medical and biological applications. *Adv. Drug Delivery Rev.* 61, 953–964.
- (5) Algar, W. R., Susumu, K., Delehanty, J. B., and Medintz, I. L. (2011) Semiconductor quantum dots in bioanalysis: crossing the valley of death. *Anal. Chem.* 83, 8826–8837.
- (6) Rosenthal, S. J., Chang, J. C., Kovtun, O., McBride, J. R., and Tomlinson, I. D. (2011) Biocompatible quantum dots for biological applications. *Chem. Biol. (Oxford, U. K.)* 18, 10–24.
- (7) Jin, Z., and Hildebrandt, N. (2012) Semiconductor quantum dots for in vitro diagnostics and cellular imaging. *Trends Biotechnol.* 30, 394–403.
- (8) Delehanty, J. B., Bradburne, C. E., Susumu, K., Boeneman, K., Mei, B. C., Farrell, D., Blanco-Canosa, J. B., Dawson, P. E., Mattoussi, H., and Medintz, I. L. (2011) Spatiotemporal multicolor labeling of individual cells using peptide-functionalized quantum dots and mixed delivery techniques. *J. Am. Chem. Soc.* 133, 10482–10489.
- (9) Clapp, A. R., Pons, T., Medintz, I. L., Delehanty, J. B., Melinger, J. S., Tiefenbrunn, T., Dawson, P. E., Fisher, B. R., O'Rourke, B., and Mattoussi, H. (2007) Two-photon excitation of quantum dot-based fluorescence resonance energy transfer and its applications. *Adv. Mater. (Weinheim, Ger.)* 19, 1921–1926.
- (10) Larson, D. R., Zipfel, W. R., Williams, R. M., Clark, S. W., Bruchez, M. P., Wise, F. W., and Webb, W. W. (2003) Water-soluble quantum dots for multiphoton fluorescence imaging in vivo. *Science* 300, 1434–1437.
- (11) Sapsford, K. E., Berti, L., and Medintz, I. L. (2006) Materials for fluorescence resonance energy transfer analysis: beyond traditional donor–acceptor combinations. *Angew. Chem. Int. Ed. Engl.* 45, 4562–4589.
- (12) Algar, W. R., Wegner, D., Huston, A. L., Blanco-Canosa, J. B., Stewart, M. H., Armstrong, A., Dawson, P. E., Hildebrandt, N., and Medintz, I. L. (2012) Quantum dots as simultaneous acceptors and donors in time-gated Förster resonance energy transfer relays: characterization and biosensing. *J. Am. Chem. Soc.* 134, 1876–1891.
- (13) Hildebrandt, N., and Geissler, D. (2012) Semiconductor quantum dots as FRET acceptors for multiplexed diagnostics and molecular ruler application. *Adv. Exp. Med. Biol.* 733, 75–86.
- (14) Resch-Genger, U., Grabolle, M., Cavaliere-Jaricot, S., Nitschke, R., and Nann, T. (2008) Quantum dots versus organic dyes as fluorescent labels. *Nat. Methods* 5, 763–775.
- (15) Delehanty, J. B., Mattoussi, H., and Medintz, I. L. (2009) Delivering quantum dots into cells: strategies, progress and remaining issues. *Anal. Bioanal. Chem.* 393, 1091–1105.
- (16) Delehanty, J. B., Susumu, K., Manthe, R. L., Algar, W. R., and Medintz, I. L. (2012) Active cellular sensing with quantum dots: transitioning from research tool to reality; a review. *Anal. Chim. Acta* 750, 63–81.
- (17) Algar, W. R., Prasuhn, D. E., Stewart, M. H., Jennings, T. L., Blanco-Canosa, J. B., Dawson, P. E., and Medintz, I. L. (2011) The controlled display of biomolecules on nanoparticles: a challenge suited to bioorthogonal chemistry. *Bioconjugate Chem.* 22, 825–858.
- (18) Chen, N., He, Y., Su, Y., Li, X., Huang, Q., Wang, H., Zhang, X., Tai, R., and Fan, C. (2012) The cytotoxicity of cadmium-based quantum dots. *Biomaterials* 33, 1238–1244.
- (19) Male, K. B., Lachance, B., Hrapovic, S., Sunahara, G., and Luong, J. H. (2008) Assessment of cytotoxicity of quantum dots and gold nanoparticles using cell-based impedance spectroscopy. *Anal. Chem.* 80, 5487–5493.
- (20) Chan, W. H., Shiao, N. H., and Lu, P. Z. (2006) CdSe quantum dots induce apoptosis in human neuroblastoma cells via mitochondrial-dependent pathways and inhibition of survival signals. *Toxicol. Lett.* 167, 191–200.
- (21) Kirchner, C., Liedl, T., Kudera, S., Pellegrino, T., Munoz Javier, A., Gaub, H. E., Stolzle, S., Fertig, N., and Parak, W. J. (2005) Cytotoxicity of colloidal CdSe and CdSe/ZnS nanoparticles. *Nano Lett.* 5, 331–338.
- (22) Cho, S. J., Maysinger, D., Jain, M., Roder, B., Hackbarth, S., and Winnik, F. M. (2007) Long-term exposure to CdTe quantum dots causes functional impairments in live cells. *Langmuir* 23, 1974–1980.
- (23) Li, K. G., Chen, J. T., Bai, S. S., Wen, X., Song, S. Y., Yu, Q., Li, J., and Wang, Y. Q. (2009) Intracellular oxidative stress and cadmium ions release induce cytotoxicity of unmodified cadmium sulfide quantum dots. *Toxicol. in Vitro* 23, 1007–1013.
- (24) Mei, B. C., Susumu, K., Medintz, I. L., Delehanty, J. B., Mountziaris, T. J., and Mattoussi, H. (2008) Modular poly(ethylene glycol) ligands for biocompatible semiconductor and gold nanocrystals with extended pH and ionic stability. *J. Mater. Chem.* 18, 1–11.
- (25) Uyeda, H. T., Medintz, I. L., Jaiswal, J. K., Simon, S. M., and Mattoussi, H. (2005) Synthesis of compact multidentate ligands to prepare stable hydrophilic quantum dot fluorophores. *J. Am. Chem. Soc.* 127, 3870–3878.
- (26) Susumu, K., Mei, B. C., and Mattoussi, H. (2009) Multifunctional ligands based on dihydrolipoic acid and poly(ethylene glycol) to promote biocompatibility of quantum dots. *Nat. Protoc.* 4, 424–436.
- (27) Susumu, K., Uyeda, H. T., Medintz, I. L., Pons, T., Delehanty, J. B., and Mattoussi, H. (2007) Enhancing the stability and biological functionalities of quantum dots via compact multifunctional ligands. *J. Am. Chem. Soc.* 129, 13987–13996.
- (28) Hoshino, A., Fujioka, K., Oku, T., Suga, M., Sasaki, Y. F., Ohta, T., Yasuhara, M., Suzuki, K., and Yamamoto, K. (2004) Physicochemical properties and cellular toxicity of nanocrystal quantum dots depend on their surface modification. *Nano Lett.* 4, 2163–2169.
- (29) Ryman-Rasmussen, J. P., Riviere, J. E., and Monteiro-Riviere, N. A. (2007) Surface coatings determine cytotoxicity and irritation potential of quantum dot nanoparticles in epidermal keratinocytes. *J. Invest. Dermatol.* 127, 143–153.
- (30) Hoshino, A., Manabe, N., Fujioka, K., Suzuki, K., Yasuhara, M., and Yamamoto, K. (2007) Use of fluorescent quantum dot bioconjugates for cellular imaging of immune cells, cell organelle labeling, and nanomedicine: surface modification regulates biological function, including cytotoxicity. *J. Artif. Organs* 10, 149–157.
- (31) Hoshino, A., Hanada, S., and Yamamoto, K. (2011) Toxicity of nanocrystal quantum dots: the relevance of surface modifications. *Arch. Toxicol.* 85, 707–720.
- (32) Hoshino, A., Fujioka, K., Oku, T., Nakamura, S., Suga, M., Yamaguchi, Y., Suzuki, K., Yasuhara, M., and Yamamoto, K. (2004) Quantum dots targeted to the assigned organelle in living cells. *Microbiol. Immunol.* 48, 985–994.

- (33) Delehanty, J. B., Bradburne, C. E., Boeneman, K., Susumu, K., Farrell, D., Mei, B. C., Blanco-Canosa, J. B., Dawson, G., Dawson, P. E., Mattoussi, H., and Medintz, I. L. (2010) Delivering quantum dot-peptide bioconjugates to the cellular cytosol: escaping from the endolysosomal system. *Integr. Biol.* 2, 265–277.
- (34) Susumu, K., Oh, E., Delehanty, J. B., Blanco-Canosa, J. B., Johnson, B. J., Jain, V., Hervey, W. J., Algar, W. R., Boeneman, K., Dawson, P. E., and Medintz, I. L. (2011) Multifunctional compact zwitterionic ligands for preparing robust biocompatible semiconductor quantum dots and gold nanoparticles. *J. Am. Chem. Soc.* 133, 9480–9496.
- (35) Winnik, F. M., and Maysinger, D. (2013) Quantum dot cytotoxicity and ways to reduce it. *Acc. Chem. Res.* 46, 672–680.
- (36) Nagy, A., Steinbrück, A., Gao, J., Doggett, N., Hollingsworth, J. A., and Iyer, R. (2012) Comprehensive analysis of the effects of CdSe quantum dot size, surface charge, and functionalization on primary human lung cells. *ACS Nano* 6, 4748–4762.
- (37) Zhang, T., Stilwell, J. L., Gerion, D., Ding, L., Elboudwarej, O., Cooke, P. A., Gray, J. W., Alivisatos, A. P., and Chen, F. F. (2006) Cellular effect of high doses of silica-coated quantum dot profiled with high throughput gene expression analysis and high content cellomics measurements. *Nano Lett.* 6, 800–808.
- (38) Sapsford, K. E., Tyner, K. M., Dair, B. J., Deschamps, J. R., and Medintz, I. L. (2011) Analyzing nanomaterial bioconjugates: a review of current and emerging purification and characterization techniques. *Anal. Chem.* 83, 4453–4488.
- (39) Marnett, L. J. (2009) Nanotoxicology—a new frontier. *Chem. Res. Toxicol.* 22, 1491.
- (40) Haugland, R. P. (2005) *The Handbook. A Guide to Fluorescent Probes and Labeling Technologies*, 10th ed.; Invitrogen: San Diego.
- (41) Alford, R., Simpson, H. M., Duberman, J., Hill, G. C., Ogawa, M., Regino, C., Kobayashi, H., and Choyke, P. L. (2009) Toxicity of organic fluorophores used in molecular imaging: literature review. *Mol. Imaging* 8, 341–354.
- (42) Albanese, A., Tang, P. S., and Chan, W. C. (2012) The effect of nanoparticle size, shape, and surface chemistry on biological systems. *Annu. Rev. Biomed. Eng.* 14, 1–16.
- (43) Delehanty, J. B., Medintz, I. L., Pons, T., Brunel, F. M., Dawson, P. E., and Mattoussi, H. (2006) Self-assembled quantum dot-peptide bioconjugates for selective intracellular delivery. *Bioconjugate Chem.* 17, 920–927.
- (44) Medintz, I. L., Pons, T., Delehanty, J. B., Susumu, K., Brunel, F. M., Dawson, P. E., and Mattoussi, H. (2008) Intracellular delivery of quantum dot-protein cargos mediated by cell penetrating peptides. *Bioconjugate Chem.* 19, 1785–1795.
- (45) Medintz, I. L., Stewart, M. H., Trammell, S. A., Susumu, K., Delehanty, J. B., Mei, B. C., Melinger, J. S., Blanco-Canosa, J. B., Dawson, P. E., and Mattoussi, H. (2010) Quantum-dot/dopamine bioconjugates function as redox coupled assemblies for in vitro and intracellular pH sensing. *Nat. Mater.* 9, 676–684.
- (46) Mattoussi, H., Mauro, J. M., Goldman, E. R., Anderson, G. P., Sundar, V. C., Mikulec, F. V., and Bawendi, M. G. (2000) Self-assembly of CdSe-ZnS quantum dot bioconjugates using an engineered recombinant protein. *J. Am. Chem. Soc.* 122, 12142–12150.
- (47) Mei, B. C., Susumu, K., Medintz, I. L., and Mattoussi, H. (2009) Polyethylene glycol-based bidentate ligands to enhance quantum dot and gold nanoparticle stability in biological media. *Nat. Protoc.* 4, 412–423.
- (48) Li, L., Yang, L., and Kotin, R. M. (2005) The DNA minor groove binding agents Hoechst 33258 and 33342 enhance recombinant adeno-associated virus (rAAV) transgene expression. *J. Gene Med.* 7, 420–431.
- (49) Nafisi, S., Saboury, A. A., Keramat, N., Neault, J. F., and Tajmir-Riahi, H. A. (2007) Stability and structural features of DNA intercalation with ethidium bromide, acridine orange and methylene blue. *J. Mol. Struct.* 827, 35–43.
- (50) Poot, M., Kavanagh, T. J., Kang, H. C., Haugland, R. P., and Rabinovitch, P. S. (1991) Flow cytometric analysis of cell cycle-dependent changes in cell thiol level by combining a new laser dye with Hoechst 33342. *Cytometry* 12, 184–187.
- (51) Cumberledge, S., and Krasnow, M. A. (1993) Intercellular signalling in *Drosophila* segment formation reconstructed in vitro. *Nature* 363, 549–552.
- (52) Burghardt, R. C., Barhoumi, R., Lewis, E. H., Bailey, R. H., Pyle, K. A., Clement, B. A., and Phillips, T. D. (1992) Patulin-induced cellular toxicity: a vital fluorescence study. *Toxicol. Appl. Pharmacol.* 112, 235–244.
- (53) Waite, J. C., Leiner, I., Lauer, P., Rae, C. S., Barbet, G., Zheng, H., Portnoy, D. A., Pamer, E. G., and Dustin, M. L. (2011) Dynamic imaging of the effector immune response to *Listeria* infection in vivo. *PLoS Pathog.* 7, e1001326.
- (54) Shrestha, S. P., Tomita, T., Weiss, L. M., and Orlofsky, A. (2006) Proliferation of *Toxoplasma gondii* in inflammatory macrophages in vivo is associated with diminished oxygen radical production in the host cell. *Int. J. Parasitol.* 36, 433–441.
- (55) Brinkley, M. (1992) A brief survey of methods for preparing protein conjugates with dyes, haptens, and cross-linking reagents. *Bioconjugate Chem.* 3, 2–13.
- (56) Rink, T. J., Tsien, R. Y., and Pozzan, T. (1982) Cytoplasmic pH and free Mg^{2+} in lymphocytes. *J. Cell Biol.* 95, 189–196.
- (57) Chan, W. H., and Shiao, N. H. (2008) Cytotoxic effect of CdSe quantum dots on mouse embryonic development. *Acta Pharmacol. Sin.* 29, 259–266.
- (58) Hoshino, A., Hanada, S., Manabe, N., Nakayama, T., and Yamamoto, K. (2009) Immune response induced by fluorescent nanocrystal quantum dots in vitro and in vivo. *IEEE Trans. NanoBioscience* 8, 51–57.
- (59) Prasad, B. R., Nikolskaya, N., Connolly, D., Smith, T. J., Byrne, S. J., Gerard, V. A., Gun'ko, Y. K., and Rochev, Y. (2010) Long-term exposure of CdTe quantum dots on PC12 cellular activity and the determination of optimum non-toxic concentrations for biological use. *J. Nanobiotechnol.* 8, 10.1186/1477-3155-8-7.
- (60) Biju, V., Muraleedharan, D., Nakayama, K., Shinohara, Y., Itoh, T., Baba, Y., and Ishikawa, M. (2007) Quantum dot-insect neuropeptide conjugates for fluorescence imaging, transfection, and nucleus targeting of living cells. *Langmuir* 23, 10254–10261.
- (61) Lewinski, N., Colvin, V., and Drezek, R. (2008) Cytotoxicity of nanoparticles. *Small* 4, 26–49.
- (62) Sapsford, K. E., Pons, T., Medintz, I. L., Higashiyama, S., Brunel, F. M., Dawson, P. E., and Mattoussi, H. (2007) Kinetics of metal-affinity driven self-assembly between proteins or peptides and CdSe-ZnS quantum dots. *J. Phys. Chem. C* 111, 11528–11538.
- (63) Prasuhn, D. E., Deschamps, J. R., Susumu, K., Stewart, M. H., Boeneman, K., Blanco-Canosa, J. B., Dawson, P. E., and Medintz, I. L. (2010) Polyvalent display and packing of peptides and proteins on semiconductor quantum dots: predicted versus experimental results. *Small* 6, 555–564.
- (64) Wiener, E., and Levanon, D. (1968) Macrophage cultures: an extracellular esterase. *Science* 159, 217.
- (65) Jobsis, P. D., Rothstein, E. C., and Balaban, R. S. (2007) Limited utility of acetoxymethyl (AM)-based intracellular delivery systems in vivo: interference by extracellular esterases. *J. Microsc.* 226, 74–81.
- (66) Athanasiou, K. A., Niederauer, G. G., and Agrawal, C. M. (1996) Sterilization, toxicity, biocompatibility and clinical applications of polylactic acid/polyglycolic acid copolymers. *Biomaterials* 17, 93–102.
- (67) Delehanty, J. B., Boeneman, K., Bradburne, C. E., Robertson, K., and Medintz, I. L. (2009) Quantum dots: a powerful tool for understanding the intricacies of nanoparticle-mediated drug delivery. *Expert Opin. Drug Delivery* 6, 1091–1112.
- (68) Delehanty, J. B., Boeneman, K., Bradburne, C. E., Robertson, K., Bongard, J. E., and Medintz, I. L. (2010) Peptides for specific intracellular delivery and targeting of nanoparticles: implications for developing nanoparticle-mediated drug delivery. *Ther. Delivery* 1, 411–433.
- (69) Rozenzhak, S. M., Kadakia, M. P., Caserta, T. M., Westbrook, T. R., Stone, M. O., and Naik, R. R. (2005) Cellular internalization and

targeting of semiconductor quantum dots. *Chem. Commun.* 17, 2217–2219.

(70) Derfus, A. M., Chan, W. C. W., and Bhatia, S. N. (2004) Intracellular delivery of quantum dots for live cell labeling and organelle tracking. *Adv. Mater.* 16, 961–966.

(71) Voura, E. B., Jaiswal, J. K., Mattoussi, H., and Simon, S. M. (2004) Tracking metastatic tumor cell extravasation with quantum dot nanocrystals and fluorescence emission-scanning microscopy. *Nat. Med.* 10, 993–998.

(72) Rodriguez-Fragoso, P., Reyes-Esparza, J., Leon-Buitimea, A., and Rodriguez-Fragoso, L. (2012) Synthesis, characterization and toxicological evaluation of maltodextrin capped cadmium sulfide nanoparticles in human cell lines and chicken embryos. *J. Nanobiotechnol.* 10, 10.1186/1477-3155-10-47.

(73) Lullmann-Rauch, R., and Ziegenhagen, M. (1991) Acridine orange, a precipitant for sulfated glycosaminoglycans, causes mucopolysaccharidosis in cultured fibroblasts. *Histochemistry* 95, 263–268.

(74) Kusuzaki, K., Takeshita, H., Murata, H., Hashiguchi, S., Nozaki, T., Emoto, K., Ashihara, T., and Hirasawa, Y. (2001) Acridine orange induces binucleation in chondrocytes. *Osteoarthr. Cartilage* 9, 147–151.

(75) Chazotte, B. (2008) Labeling lysosomes in live cells with fluorescent dyes for imaging. *Cold Spring Harbor Protocols* 2008, pdb.prot4929.

(76) Bhakdi, S. C., Sratongno, P., Chimma, P., Rungruang, T., Chuncharunee, A., Neumann, H. P. H., Malasit, P., and Pattanapanyasat, K. (2007) Re-evaluating acridine orange for rapid flow cytometric enumeration of parasitemia in malaria-infected rodents. *Cytometry Part A* 71A, 662–667.

(77) Morris, M. C., Gros, E., Aldrian-Herrada, G., Choob, M., Archdeacon, J., Heitz, F., and Divita, G. (2007) A non-covalent peptide-based carrier for in vivo delivery of DNA mimics. *Nucleic Acids Res.* 35, 10.1093/nar/gkm053.

(78) Sethuraman, V. A., Lee, M. C., and Bae, Y. H. (2008) A biodegradable pH-sensitive micelle system for targeting acidic solid tumors. *Pharm. Res.* 25, 657–666.

(79) Koren, E., and Torchilin, V. P. (2012) Cell-penetrating peptides: breaking through to the other side. *Trends Mol. Med.* 18, 385–393.

(80) Madani, F., Lindberg, S., Langel, U., Futaki, S., and Graslund, A. (2011) Mechanisms of cellular uptake of cell-penetrating peptides. *J. Biophys.* 10, 10.1155/2011/414729.

(81) Qi, L., and Gao, X. (2008) Quantum dot–amphipol nanocomplex for intracellular delivery and real-time imaging of siRNA. *ACS Nano* 2, 1403–1410.

(82) Landry, J. J. M., Pyl, P. T., Rausch, T., Zichner, T., Tekkedil, M. M., Stütz, A. M., Jauch, A., Aiyar, R. S., Pau, G., Delhomme, N., Gagneur, J., Korbel, J. O., Huber, W., and Steinmetz, L. M. (2013) The genomic and transcriptomic landscape of a HeLa cell line. *G3: Genes, Genomes, Genet.*, DOI: 10.1534/g3.113.005777.

(83) Freshney, R. I. (2010) *Culture of animal cells: a manual of basic technique and specialized applications*, 6th ed., Wiley-Blackwell, Hoboken.

(84) Park, S., and Hamad-Schifferli, K. (2010) Nanoscale interfaces to biology. *Curr. Opin. Chem. Biol.* 14, 616–622.

(85) Nel, A. E., Madler, L., Velegol, D., Xia, T., Hoek, E. M. V., Somasundaran, P., Klaessig, F., Castranova, V., and Thompson, M. (2009) Understanding biophysicochemical interactions at the nano-bio interface. *Nat. Mater.* 8, 543–557.

(86) Lynch, I., Cedervall, T., Lundqvist, M., Cabaleiro-Lago, C., Linse, S., and Dawson, K. A. (2007) The nanoparticle–protein complex as a biological entity; a complex fluids and surface science challenge for the 21st century. *Adv. Colloid Interface Sci.* 134–135, 167–174.

(87) Walkey, C. D., Olsen, J. B., Guo, H., Emili, A., and Chan, W. C. W. (2011) Nanoparticle size and surface chemistry determine serum protein adsorption and macrophage uptake. *J. Am. Chem. Soc.* 134, 2139–2147.

(88) Mattoussi, H., Palui, G., and Na, H. B. (2012) Luminescent quantum dots as platforms for probing *in vitro* and *in vivo* biological processes. *Adv. Drug Delivery Rev.* 64, 138–166.

(89) Hotzer, B., Medintz, I. L., and Hildebrandt, N. (2012) Fluorescence in nanobiotechnology: sophisticated fluorophores for novel applications. *Small* 8, 2297–2326.

(90) Iversen, T. G., Skotland, T., and Sandvig, K. (2011) Endocytosis and intracellular transport of nanoparticles: present knowledge and need for future studies. *Nano Today* 6, 176–185.

(91) Symens, N., Soenen, S. J., Rejman, J., Braeckmans, K., De Smedt, S. C., and Remaut, K. (2012) Intracellular partitioning of cell organelles and extraneous nanoparticles during mitosis. *Adv. Drug Delivery Rev.* 64, 78–94.

(92) Clapp, A. R., Goldman, E. R., and Mattoussi, H. (2006) Capping of CdSe-ZnS quantum dots with DHLA and subsequent conjugation with proteins. *Nat. Protoc.* 1, 1258–1266.

(93) Schnolzer, M., Alewood, P., Jones, A., Alewood, D., and Kent, S. B. (1992) In situ neutralization in Boc-chemistry solid phase peptide synthesis. Rapid, high yield assembly of difficult sequences. *Int. J. Pept. Protein. Res.* 40, 180–193.

(94) Sapsford, K. E., Farrell, D., Sun, S., Rasooly, A., Mattoussi, H., and Medintz, I. L. (2009) Monitoring of enzymatic proteolysis on an electrochemiluminescent-CCD microchip platform using quantum dot-peptide substrates. *Sens. & Act. B: Chem.* 139, 13–21.

(95) Berridge, M. V., and Tan, A. S. (1993) Characterization of the cellular reduction of 3-(4,5-dimethylthiazol-2-yl)-2,5-diphenyltetrazolium bromide (MTT): subcellular localization, substrate dependence, and involvement of mitochondrial electron transport in MTT reduction. *Arch. Biochem. Biophys.* 303, 474–482.

(96) Berridge, M. V., Herst, P. M., and Tan, A. S. (2005) Tetrazolium dyes as tools in cell biology: new insights into their cellular reduction. *Biotechnol. Annu. Rev.* 11, 127–152.